The Hall effect in a classical two-dimensional electron gas without electrical contacts



1993 J. Phys.: Condens. Matter 5 3587

(http://iopscience.iop.org/0953-8984/5/22/010)

J. Phys.: Condens. Matter 5 (1993) 3587–3592. Printed in the UK

# The Hall effect in a classical two-dimensional electron gas without electrical contacts

P J M Peters†, M J Lea‡, W P N M Jacobs†, J F A Nijs† and R W van der Heijden†

† Department of Physics, Eindhoven University of Technology, PO Box 513, 5600 MB Eindhoven, The Netherlands

‡ Department of Physics, Royal Holloway, University of London, Egham, Surrey TW20 0EX, UK

Received 16 February 1993, in final form 29 March 1993

**Abstract.** Measurements of the phase shift between current and voltage as a function of magnetic field are reported for electrodes in an array which are capacitively coupled to the two-dimensional electron gas on liquid helium. It is experimentally shown that the phase of the current at the extreme edge of the sample decreases with magnetic field when the Hall angle comes close to 90°. It is shown that this is a direct consequence of the unusual condition of total charge conservation for an electrically isolated sample.

## 1. Introduction

A strong magnetic field imposed on a high-mobility electron system drastically modifies the current distribution and equipotential lines in the plane normal to the magnetic field [1]. The distortion arises because the Hall angle $\beta$ ($\beta = \tan^{-1}(\mu B)$ with $\mu$ the mobility and $B$ the magnetic field) becomes close to 90° for $\mu B \gg 1$. This regime is nowadays extremely important as it is easily reached in two-dimensional electron systems such as inversion layers, heterojunctions or electrons on liquid helium. A conventional DC Hall effect measurement utilizes (at least) two current contacts at different positions on the sample that short the Hall field near these contacts. In the ideal case, where the Hall angle is equal to 90°, as occurs under quantum Hall effect conditions, one part of the edge of the sample (including one current contact) is at one potential, while the other part (including the other contact) is at another potential [2]. The difference is equal to the (quantized) Hall voltage, which can be measured at any two terminals at opposite sides [3]. At the connection of the two sides, in the corners of the sample, the electric field has a power law singularity [4] where the dissipation occurs.

The situation is very different when there are no electrical contacts to the two-dimensional electron system (2DES). Such systems can be driven by AC techniques, for instance by capacitive coupling. At low fields, $\mu B \ll 1$, the AC Hall effect is equivalent to the DC Hall effect. At sufficiently large fields and frequencies, it leads to a localized edge mode [5], which in general is a weakly damped propagating wave called an edge magnetoplasmon, which can be regarded as a dynamic Hall effect [6]. Edge magnetoplasmons have been investigated recently in both the 2DES in semiconductors [7] and electrons on liquid helium [8, 9]. In these experiments edge magnetoplasmon resonances were measured, where the sample circumference is an integral multiple of the wavelength.

0953-8984/93/223587+06$07.50  

Non-resonant behaviour, where both the wavelength and damping length are smaller than the sample circumference, has been observed for electrons on helium [9].

In this paper, we investigate experimentally and theoretically the AC Hall effect for the non-degenerate 2DES of electrons on liquid helium. The magnetic fields are high enough that edge mode formation is important. The frequencies are chosen low enough, however, that the wavelength of the edge mode is larger than the sample circumference. These conditions correspond to the DC Hall effect regime at large Hall angles. The important difference is the absence, for the capacitively coupled case, of current contacts that provide severe potential boundary value conditions with their drastic consequences for the equipotential and current lines distribution. It is found that the potential is nearly constant all around the edge. Its magnetic-field-dependent value is determined by the property that the total charge in the sheet is constant. An unambiguous and distinct experimental signature of this charge conservation condition is reported.

## 2. Experimental details

The electron layer is held between two metal plates separated by 3 mm. The lower one, shown in the inset to figure 1, consists of an array of electrodes situated 0.5 mm below the liquid surface. The electrodes couple capacitively to the electron sheet at the surface. One of the lower electrodes (usually 1) is driven by an AC voltage $v\cos(\omega t)$. Using a lock-in amplifier, the components of the currents in and out of phase with respect to the driving voltage, $I(0°)$ and $I(90°)$, are measured at the electrode diametrically opposite to the driving electrode. The phase of the current is defined as $\Phi = \pi/2 - \tan^{-1}[I(90°)/I(0°)]$ so that pure capacitive coupling (i.e. a perfectly conducting electron sheet in zero magnetic field) would correspond to $\Phi = 0$ [10]. The currents measured with the surface uncharged, which are due to stray capacitance and leakage resistance, are subtracted from the signal currents.

## 3. Results and analysis

A typical set of data is given in figure 1, which shows the measured phase at a fixed density as a function of magnetic field for three frequencies at a temperature of 1.9 K at which $\mu \simeq 2\ \mathrm{m^2\ V^{-1}\ s^{-1}}$. Data at fixed frequency, but different densities, are similar. The measured absolute values of the phase have a systematic error (due to instrumental phase shifts) that causes for instance the small negative phase at zero field in curve (a) in figure 1. The feature of interest is the decrease in phase at low fields, which is only observed when the electron pool slightly overlaps with the electrodes involved, 1 and 5 in this case. The pool radius was controlled by the voltage on a cylindrical guard surrounding the pool. Consequently, no such decrease was observed when the electrodes 3–7, which extend deeper into the pool, were used as generator and detector.

In the Sommer–Tanner analysis [10], the phase change is proportional to the resistance of the electron sheet, so that a similar decreasing phase has previously been interpreted as a negative magnetoresistance, due to weak localization [11]. It is now clear that the original analysis only applies in zero magnetic field or for $\mu B \ll 1$ or for a circularly symmetric electrode geometry [12]. We now show that a decrease in phase at the edges of a 2DES is characteristic of the AC Hall effect, and will always be measured at one of the Hall electrodes (3 or 7, depending on the field direction with 1 driven) even in small fields. However, for large electrodes extending significantly into the pool, a positive phase shift will be observed on all other electrodes [13].

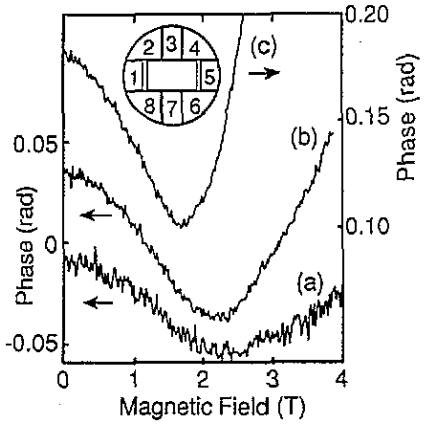


**Figure 1.** Inset: geometry of the experimental electrode array. Electrodes 1 and 5 are separated by 12 mm, electrodes 3 and 7 by 6 mm. Array diameter is 19 mm and a cylindrical guard of 19 mm diameter surrounds the pool. Curves (a), (b) and (c) give the measured phase of the current at electrode 5 with electrode 1 driven, at frequencies of 1.01, 2.02 and 4.04 kHz respectively, for an electron density of $4.2 \times 10^{11}$ m$^{-2}$ and temperature of 1.9 K. The calculated radius of the pool is 7.4 mm. Assuming a mobility of 2 m$^2$ V$^{-1}$ s$^{-1}$, the $\delta_\parallel$ parameters for curves (a), (b) and (c) are 44, 31 and 22 mm respectively.

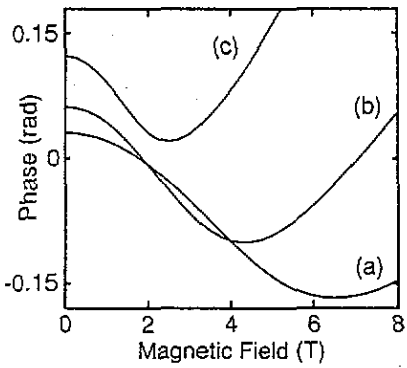


**Figure 2.** Calculated electrode-averaged current phase shifts for the same parameters as in figure 1, with corresponding curve labelling.

The response of the system can be analysed to a good approximation by the 2D diffusion equation [14]:

$$\partial^2 V(\boldsymbol{r})/\partial x^2 + \partial^2 V(\boldsymbol{r})/\partial y^2 = \left(\mathrm{j}\omega C_s/\sigma_{xx}\right)(V(\boldsymbol{r}) - v(\boldsymbol{r})) \tag{1}$$

where $V(\boldsymbol{r})$ is the AC potential in the sheet, $\omega$ the angular frequency, $C_s$ the geometric capacitance per unit area between sheet and screening electrodes, $\sigma_{xx}$ the diagonal component of the magnetoconductivity tensor and $v(\boldsymbol{r})$ the amplitude of the external voltage on the electrodes (constant on a driven electrode, zero elsewhere). For the purpose of the present paper, it suffices to assume rigid boundaries and a homogeneous rectangular density profile. The real, inhomogeneous profile is, however, important for a complete description of the edge mode in higher fields [9].

For a semi-infinite sheet, the solution of (1) with $v = 0$, subject to the boundary condition that the current density at the edge is zero perpendicular to the edge, is $V = V_0 \exp[\mathrm{j}(\omega t - \boldsymbol{k} \cdot \boldsymbol{r})]$, where $V_0$ is a constant [14]. The components of $\boldsymbol{k}$ parallel and perpendicular to the edge are $k_\parallel = (1 - \mathrm{j})/\delta_\parallel$ and $k_\perp = (1 - \mathrm{j})/\delta_\perp$ with $\delta_\parallel = (2/\rho_{xx}\omega C_s)^{1/2}$ and $\delta_\perp = (\rho_{xx}/\rho_{xy})\delta_\parallel$ with $\rho_{xx}$ and $\rho_{xy}$ the diagonal and off-diagonal components of the magnetoresistivity tensor. The solution is therefore characterized by two length parameters $\delta_\parallel$, giving the decay length along the edge, and $\delta_\perp$, giving the decay perpendicular to the edge. Note that under the conditions used of complete screening and sharp profiles, the excitation is strongly damped, i.e. the propagation constants $k_\parallel$ and $k_\perp$ have equal real and imaginary parts [5]. This analytical solution for the semi-infinite sheet is very helpful for understanding the results of numerical calculations for the finite system.

For the finite, driven system, equation (1) is solved numerically for the particular electrode geometry, using the method described in [14]. The experimentally measured parameter, the current at the detecting electrode, is obtained from $I = \int\int \mathrm{j}\omega C_s V(\boldsymbol{r})\,\mathrm{d}A$,

where the integration is over the detecting electrode. There is no *a priori* constraint on the potentials anywhere in the sheet, unlike in the more conventional, contacted case where the potentials at the current contacts are fixed. As a consequence, for the present electrically isolated system, the total charge remains constant, or equivalently, the sum of the charge variations $\Delta n_\omega$ must be zero. In the capacitively coupled model [14], the charge variation $\Delta n_\omega$ is related to the potential variations by $e\Delta n_\omega = C_s(V - v)$. Using $\int\int \Delta n_\omega \, dA = 0$ then leads to

$$\int\int V(r)\, dA = vA_{ex} \tag{2}$$

where integration is over the sheet surface and $A_{ex}$ is the area of the exciting electrode. Since $v$ is real, equation (2) implies that the average of $\mathrm{Im}(V(r))$ is zero. At zero field and long wavelengths, so that $V(r)$ is approximately constant, equation (2) can be interpreted as the capacitive voltage divider between the voltage at the exciting electrode and the voltage of the sheet.

The results of the numerical calculations are given in figure 2 for the values of the parameter $\delta_\parallel$ that correspond to the experiments of figure 1. Here the simple Drude model is used for the transport parameters $\rho_{xx} = 1/ne\mu$ (independent of magnetic field) and $\rho_{xy} = B/ne$ ($n$ is the charge density and $e$ the elementary charge). The decreasing phase is nicely reproduced by the calculations. Also in the calculations it is found only when the pool has a small overlap with the electrodes. Using the electrode combination 3–7, leaving all other parameters unchanged, no decreasing phase is found in the calculations, which strikingly corroborates the experimental findings. Roughly, the effect sets in when $\delta_\perp \leqslant \delta_\parallel$ or equivalently, in the Drude model, when $\mu B \geqslant 1$. In the numerical calculations it is seen that the position of the minimum occurs for nearly the same $\delta_\perp$ in all cases ($\delta_\perp = \delta_\parallel/\mu B$ in the Drude model). At the minimum, $\delta_\perp \simeq 4$ mm, which is of the order of the pool radius (7.4 mm).

From the numerical results it follows that the decreasing phase would be best observed (and understood) when $\delta_\parallel$ is much larger than the pool size and $\delta_\perp$ is of the order of the pool size. This combination implies large magnetic fields. Experimentally however, magnetoresistance [15] which strongly decreases $\delta_\parallel$, will completely obscure the minimum at strong fields, so that a medium field strength (and $\delta$ parameters) as well as a high temperature must be used as a compromise. Magnetoresistance also causes the quantitative differences between experiment and calculations (note the different horizontal scales in figures 1 and 2), but these will not be further discussed in this paper.

A better understanding of the decreasing-phase phenomenon may be obtained by considering the detailed behaviour of $V$ across the pool. For a qualitative insight, it is most instructive to consider large $\delta_\parallel$-values ($\delta_\parallel \gg D$, where $D$ is the pool diameter) as this essentially contains the effect. For this purpose $V(r)$ was calculated for a $\delta_\parallel$ of 100 mm, somewhat larger than the experimental values. In figure 3, the phase of $V$ for a cross section passing through the middles of electrodes 3 and 7 (1 is driven) is given for several values of magnetic field. Referring to the semi-infinite sheet solution, along the circumference of the sheet, the variation of $V$ will be roughly given by $V_0 \exp(-jk_\parallel l)$ where $l$ is the distance along the sheet ($0 \leqslant l \leqslant \pi D$). Since we choose $D/\delta_\parallel \ll 1$ this factor will not vary very much, neither in amplitude nor in phase. Therefore *all* central cross sections give similar results as in figure 3, apart from differences of order $D/\delta_\parallel$. This was confirmed by plots along other cross sections. Figure 3 therefore represents the phase of $V$ across the sheet very well.

Referring again to the semi-infinite sheet solution, the variation of $V$ towards the centre should be given by $V_0 \exp(-jk_\perp r)$, where $r$ is the distance from the edge. The phase $\phi$

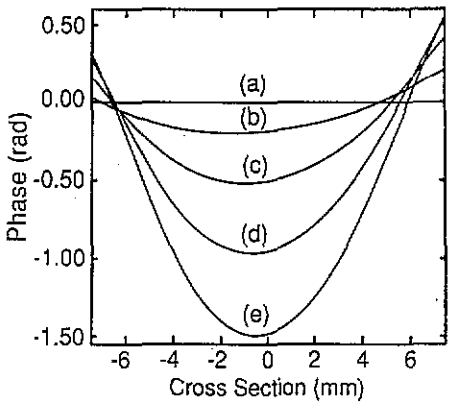


**Figure 3.** The calculated phase of the voltage $V(x, y)$ in the electron sheet along a diagonal cross section through the sheet along the direction 3–7 with electrode 1 driven (refer to inset in figure 1). The calculations are performed for $\delta_\parallel$ = 100 mm. The mobility (2 $m^2$ $V^{-1}$ $s^{-1}$), pool radius (7.4 mm, corresponding to the end points of the curves) and level height are the same as used in figures 1 and 2. Curves (a) to (e) correspond to magnetic field values of 0, 6, 10, 14, and 18 T, respectively.

of $V$ therefore decreases from the edge as $\phi = \phi_0 - r/\delta_\perp = \phi_0 - \mu B r/\delta_\parallel$, which can be verified from the slopes of the straight line portions near the edges at ±7.4mm in figure 3. The amplitude of $V$ decreases from the edge as $\exp(-r/\delta_\perp)$ (not shown). The phase $\phi_0$ at the edge ($r = 0$), is about equal to the phase of $V_0$ (apart from a factor of order $l/\delta_\parallel$). Both $\phi_0$ and the magnitude of $V_0$ are determined by equation (2), which implies that the phase of the average of $V(r)$ must be zero. The stronger decrease of $\phi$ towards the centre for larger $B$ (see figure 3) is therefore compensated by an increase in $\phi_0$, the phase at the edge. Since the amplitude of $V$ decays rapidly from the edge in large fields, $\phi_0$ will reach a limiting value as seen in figure 3. This can be seen by noting that the phase of $\int_0^\infty \exp(-jk_\perp r)\,dr$ equals $-\pi/4$. Hence the theoretical limiting value of $\phi_0$ is just $+\pi/4$.

To compare with the experimental data it should first be noted that the measured currents are proportional to $j\omega C_s V(r)$ and that the experimentally measured phase shift is defined as $\Phi = \tan^{-1}[I(0°)/I(90°)]$. Hence the phase shift $\Phi$ is *minus* the phase of the average voltage $V(r)$ over the measuring electrode. When the detecting electrode extends only slightly into the pool, it will sense the phase of $V$ near the edge, which increases with $B$, and so the phase of $I$ decreases. This is the case for electrode 5, which has only 1.5 mm overlap with the pool. When the detecting electrode extends deep into the pool (e.g. electrodes 3 and 7 which have 4.5 mm overlap, or electrode 5 when a larger pool diameter has been chosen), then the decrease in phase of $V$ in the interior will dominate the electrode-averaged signal. The measured phase of the current will then rise, and eventually stabilize near the value $D/\delta_\parallel \ll 1$ (this regime is not covered in the range displayed in figures 1 and 2). For finite electrode widths, this situation will always be met at sufficiently large fields when $\delta_\perp$ becomes of the order of the overlap with the detecting electrode. This explains why in the theoretical curves the electrode-averaged phase of the current has a minimum. As mentioned, the experimentally observed rise is dominated by magnetoresistance, which becomes important for fields above 2 T.

The analogy with the familiar DC Hall effect may be noted from figure 3. For the contactless system with $\delta_\parallel \gg D$, at large magnetic fields where $\delta_\perp \ll D$, the potential at the edge of the sample has the same value $V_0$ over the entire perimeter. Its value, magnitude and phase, is determined by condition (2). A distinct signature of this picture, the decreasing phase, has been reported in this work. In samples with current contacts at fields such that $\mu B \gg 1$, or equivalently $\rho_{xy}/\rho_{xx} \gg 1$, the potential at the edge has two distinct values at different sides of the sample with near-singularities at the connection points. The two values are equal to the externally applied potentials at the two current contacts.

In conclusion, the phenomenon reported and discussed here has features from both the

DC Hall effect and the high-field dynamic AC Hall effect or edge magnetoplasmon regime and therefore makes a bridge between these two regimes.

## Acknowledgments

We would like to thank Dr A T A M de Waele and Dr Yu P Monarkha for their interest in this work and helpful discussions, Dr A L Tal for advice on the numerical calculations and J J G M van Amelsvoort, L C van Hout and L M W Penders for technical support. We also thank the Science and Engineering Research Council (SERC, UK) for financial support. This work is part of the research program of the 'Stichting voor Fundamenteel Onderzoek der Materie (FOM)', which is financially supported by the 'Nederlandse Organisatie voor Wetenschappelijk Onderzoek (NWO)'.

## References

[1] Weiss H 1966 *Semiconductors and Semimetals* vol 1, ed R K Willardson and A C Beer (New York: Academic) ch 10, p 318
Cage M E 1987 *The Quantum Hall Effect* ed R E Prange and S M Girvin (New York: Springer) ch 2.11
[2] See e.g. figure 13c Aoki H 1987 *Rep. Prog. Phys.* **50** 655
[3] Fang F F and Stiles P J 1983 *Phys. Rev.* B **27** 6487
Rikken G L J A, van Haaren J A M M, van der Wel W, van Gelder A P, van Kempen H, Wyder P, André J P, Ploog K and Weimann G 1988 *Phys. Rev.* B **37** 6181
[4] Rendell R W and Girvin S M 1981 *Phys. Rev.* B **23** 6610
[5] Lea M J, Stone A O and Fozooni P 1988 *Europhys. Lett.* 7 641
[6] Volkov V A and Mikhailov S A 1991 *Modern Problems in Condensed Matter Sciences* vol 272, ed V M Agranovich and A A Maradudin (Amsterdam: North-Holland) ch 15, p 855
[7] Allen S J Jr, Störmer H L and Hwang J C M 1983 *Phys. Rev.* B **28** 4875
Govorkov S A, Reznikov M I, Senichkin A P and Tal'yanskii V I 1986 *Pis. Zh. Eksp. Teor. Fiz.* **44** 380 (Engl. Transl. *1986 JETP Lett.* **44** 487)
Volkov V A, Galchenkov D V, Galchenkov L A, Grodnenskii Z M, Matov O R and Mikhailov S A 1986 *Pis. Zh. Eksp. Teor. Fiz.* **44** 510 (Engl. Transl. *1986 JETP Lett.* **44** 655)
Tal'yanskii V I, Batov I E, Medvedev B K, Kotthaus J, Wassermeier M, Wixforth A, Weimann J, Schlapp W and Nikel W 1989 *Pis. Zh. Eksp. Teor. Fiz.* **50** 196 (Engl. Transl. *1989 JETP Lett.* 50 221)
Wassermeier M, Oshinowo J, Kotthaus J P, MacDonald A H, Foxon C T and Harris J J 1990 *Phys. Rev.* B **41** 10287
Grodnensky I, Heitmann D and von Klitzing K 1991 *Phys. Rev. Lett.* **67** 1019
Ashoori R C, Störmer H L, Pfeiffer L N, Baldwin K W and West K 1992 *Phys. Rev.* B **45** 3894
[8] Mast D B, Dahm A J and Fetter A L 1985 *Phys. Rev. Lett.* **54** 1706
Glattli D C, Andrei E Y, Deville G, Poitrenaud G and Williams F I B 1985 *Phys. Rev. Lett.* **54** 1710
[9] Peters P J M, Lea M J, Janssen A M L, Stone A O, Jacobs W P N M, Fozooni P and van der Heijden R W 1991 *Phys. Rev. Lett.* **67** 2199
[10] Sommer W T and Tanner D J 1971 *Phys. Rev. Lett.* **27** 1345
Mehrotra R and Dahm A J 1987 *J. Low Temp. Phys.* **67** 115
[11] Janssen A M L, van der Heijden R W, de Waele A T A M, Gijsman H M and Peeters F M 1990 *Surf. Sci.* **229** 365
[12] The observations of negative magnetoresistance made under such conditions are therefore not invalidated:
Adams P W and Paalanen M A 1987 *Phys. Rev. Lett.* **58** 2106
Adams P W 1990 *Phys. Rev. Lett.* **65** 3333
[13] Lea M J unpublished
[14] Lea M J, Stone A O, Fozooni P and Frost J 1991 *J. Low Temp. Phys.* **85** 67
[15] van der Heijden R W, van de Sanden M C M, Surewaard J H G, de Waele A T A M, Gijsman H M and Peeters F M 1988 *Europhys. Lett.* **6** 75
van der Heijden R W, Gijsman H M and Peeters F M 1988 *J. Phys. C: Solid State Phys.* **21** L1165